



Contents lists available at ScienceDirect

## Arabian Journal of Chemistry

journal homepage: [www.ksu.edu.sa](http://www.ksu.edu.sa)

# *In-vivo* metabolic profiling of the Natural products Emodin and Emodin-8-O- $\beta$ -D-glucoside in rats using liquid chromatography quadrupole Orbitrap mass spectrometry

Junqi Bai<sup>a</sup>, He Su<sup>a</sup>, Baosheng Liao<sup>a</sup>, Juan Huang<sup>a</sup>, Danchun Zhang<sup>a</sup>, Lu Gong<sup>a</sup>, Xuhua Shi<sup>a,b</sup>, Zhihai Huang<sup>a,\*</sup>, Xiaohui Qiu<sup>a,b,\*</sup>

<sup>a</sup> Guangdong Provincial Hospital of Traditional Chinese Medicine, The Second Clinical Medical College of Guangzhou University of Chinese Medicine, Guangzhou 510006, China

<sup>b</sup> Guangdong Provincial Key Laboratory of Clinical Research on Traditional Chinese Medicine Syndrome, Guangzhou 510006, China

## ARTICLE INFO

## Keywords:

Emodin  
Emodin-8-O- $\beta$ -D-glucoside  
Metabolite  
UHPLC-Q-Exactive Orbitrap MS

## ABSTRACT

Emodin (EM) and emodin-8-O- $\beta$ -D-glucoside (EG) were found in various medicinal plants such as *Rheum palmatum*, *Aloe vera*, *Polygonum multiflorum*, and *Polygonum cuspidatum*. They have different pharmacological properties and are considered potentially toxic substances. It is necessary to identify the metabolites and their distribution in the body. In this study, a comprehensive analytical strategy was developed to characterize the metabolites of EM and EG *in vivo* using UHPLC-Q-Exactive Orbitrap MS. 190 metabolites were identified in the bio-samples, in addition to the commonly reported glycoside hydrolysis, hydrogenation, hydroxylation, glucuronide conjugation, and sulfation conjugation. We also discovered new pathways such as formylation, acetylation, glycol acylation, lactation, glycerolization, malonylation, glycerol acid acylation, hydroxyvalerylation, erythroxylation, glutaric acidification, hydroxybenzoylation, glutamylation, hydroxyglutamyl, ascorbylation, aspartylglycylation, dihydroxyphenylglycylation, trihydroxyphenylglycylation, dihydroxymethoxyphenylglycylation, and ring-opening of EM. Cluster analysis revealed that each tissue in the EM and EG groups exhibited a high degree of similarity in their metabolic pathway preferences and bodily distributions, as they clustered together. Interestingly, the presence of glycol acylation, glycerolization, and glycerol acid acylation in the liver may be related to the lipid-lowering effects of EM and EG. These findings offer valuable insights for a more comprehensive understanding of the safety and efficacy of EM and EG, as well as valuable methods for metabolic characterization.

## 1. Introduction

Emodin (1, 3, 8-trihydroxy-6-methylanthraquinone) and emodin-8-O- $\beta$ -D-glucoside are present in various medicinal plants such as *Rheum palmatum*, *Aloe vera*, *Polygonum multiflorum*, and *Polygonum cuspidatum* (Wang et al., 2017; Ghimire et al., 2015; Lin et al., 2015; Li et al., 2016). It is well-known that EM and EG have similar pharmacological properties, including anti-inflammation (Park, et al., 2016; Ding et al., 2008), anti-cancer (Hsu and Chung, 2012), lipid-lowering (Su et al., 2020), neuroprotective (Leung et al., 2020), promoting bone cell proliferation and differentiation (Lee et al., 2008), neuroprotective (Wang et al.,

2007; Wang et al., 2021), cognitive enhancing effects (Mitra et al., 2022), and has broad application prospects. Meanwhile, EM and EG are also considered potential toxic substances in *Polygonum multiflorum* (Dong et al., 2016; Wang et al., 2022; Wu et al., 2018). The mechanism of drug-induced liver injury is closely related to metabolism.

There are many studies on the *in-vivo* metabolism of EM. Cheng Huiling (Cheng et al., 2020) identified 18 emodin metabolites in rat plasma through high-resolution mass spectrometry and multiple mass loss filtration, the main metabolic pathways being glucuronidation, sulfation, and hydroxylation. Chen Xuan (Tian et al., 2012) used hollow fiber liquid phase microextraction (HFLPME) coupled with high-

\* Corresponding author.

E-mail addresses: [baijunqibai@126.com](mailto:baijunqibai@126.com) (J. Bai), [suhe@gzucm.edu.cn](mailto:suhe@gzucm.edu.cn) (H. Su), [swjs082lbs@126.com](mailto:swjs082lbs@126.com) (B. Liao), [juanhuanzi@126.com](mailto:juanhuanzi@126.com) (J. Huang), [zhangdanchun@gzucm.edu.cn](mailto:zhangdanchun@gzucm.edu.cn) (D. Zhang), [gonglu0904@126.com](mailto:gonglu0904@126.com) (L. Gong), [549203216@qq.com](mailto:549203216@qq.com) (X. Shi), [zhhuang7308@163.com](mailto:zhhuang7308@163.com) (Z. Huang), [qixiaohui@gzucm.edu.cn](mailto:qixiaohui@gzucm.edu.cn) (X. Qiu).

<https://doi.org/10.1016/j.arabjc.2024.105905>

Received 10 April 2024; Accepted 8 July 2024

Available online 13 July 2024

1878-5352/© 2024 The Authors. Published by Elsevier B.V. on behalf of King Saud University. This is an open access article under the CC BY-NC-ND license (<http://creativecommons.org/licenses/by-nc-nd/4.0/>).

performance liquid chromatography (HPLC) to identify six metabolites in the plasma and urine of rats of different genders. Male rats detected more types of metabolites than female rats. Wu (Wu et al., 2017) identified the metabolites of EM in rat bile and urine. There are 13 types of emodin metabolites in bile and 22 types in urine, including 4 types of phase I and 18 types of phase II metabolites. The main metabolic pathway of emodin is glucuronidation. Lin (Lin et al., 2012) conducted a study on the tissue distribution of EM and its metabolites. It was found that emodin glucuronide and sulfation products are predominantly distributed in the lungs and kidneys, with no detection in the heart and brain. There is relatively little research on the *in vivo* metabolism of EG. We have previously published and identified a total of 47 metabolites. EG mainly undergoes hydrolysis, hydroxylation, methylation, carboxylation, glucuronidation, sulfation, and various complex reactions in rats (Shi et al., 2021).

The material basis of a drug is crucial in determining its efficacy and toxicology. Although the *in vivo* metabolites of EM and EG have been published for a long time, the toxicity of EM and EG remains unclear. With the significant improvement in modern detection sensitivity, we believe that conducting in-depth research on the *in vivo* metabolites of EM and EG is necessary to advance the process of *in vivo* metabolite analysis and gain more insights into the pharmacodynamics and toxicology of EM and EG.

## 2. Materials and methods

### 2.1. Materials

EG and Citreosein were purchased from Yuanye Bio-Technology Co., Ltd (No. T20F8Z29653, T20F8Z29653, P31010F101343, purity  $\geq 98\%$ , Shanghai, China). EM and Rhein were purchased China Institute for food and drug control (No. 110756–201913, 110757–201607, Beijing, China). Acetonitrile and methanol (HPLC grade), were supplied by E. Merck (Darmstadt, Germany), formic acid (HPLC grade) was purchased from fisher (United States), ultra-pure water was prepared by a Milli-Q water purification system (Millipore, MA, United States).

### 2.2. UHPLC-Q-Exactive plus orbitrap MS/MS analysis

#### 2.2.1. Liquid chromatography

All the samples were analyzed using an Ultimate 3000 UHPLC system (Dionex, USA) that was controlled by Thermo Xcalibur software (Thermo Fisher Scientific, USA). Samples were separated on a Waters UPLC T3 column (100\*2.1 mm, 1.7  $\mu\text{m}$ ) (Waters, USA). The mobile phase consisted of solvent A (0.1 % formic acid) and solvent B (acetonitrile). A gradient elution was performed using the following optimized gradient program: 15 ~ 30 % B at 0 ~ 1 min, 30 ~ 40 % B at 1 ~ 3 min, 40 ~ 80 % B at 3 ~ 5 min, 80 ~ 80 % B at 5 ~ 8 min, 80 ~ 15 % B at 8 ~ 9 min, 15 ~ 15 % B at 9 ~ 10 min. The flow rate was maintained at 0.2 ml/min, the sample injection volume was 5  $\mu\text{L}$ , and the column temperature was maintained at 35  $^{\circ}\text{C}$ .

#### 2.2.2. Mass spectrometry

Mass spectrometry was performed on a Q-Exactive Plus<sup>TM</sup> quadrupole-Orbitrap mass spectrometer (Thermo Fisher Scientific, USA) with heat electrospray ionization (HESI) in the negative mode. The main optimized parameters for MS were set as follows: The scan mass range was set at  $m/z$  120–1500. a full scan and fragment spectral resolution of 70,000 FWHM; capillary temperature, 350  $^{\circ}\text{C}$ ; auxiliary gas heater temperature, 350  $^{\circ}\text{C}$ ; spray voltage,  $-3.2\text{ kV}$ ; sheath gas flow rate, 40 Arb; auxiliary gas flow rate, 15 Arb; sweep gas flow rate, 0; S-lens RF level, 50. The properties of dd-MS<sup>2</sup> were as follows: resolution, 17,500; The acquisition mode of stepped NCE (normalized collision energy), 30, 50, and 70 eV. The accumulated resultant fragment ions were injected into the Orbitrap mass analyzer for single-scan detection.

### 2.3. Animals and drug administration

Male Sprague-Dawley rats (240  $\pm$  20 g) were obtained from the Laboratory Animal Center of Southern Medical University (Guangzhou, China), with a laboratory animal production license No.: SCXK (Yue) 2018–0094. All animals had ad *libitum* access to water and standard chow, and were acclimatized to the facilities for one week. The rats were housed in an air-conditioned animal facility at 23  $\pm$  2 $^{\circ}\text{C}$ , with a humidity of 55  $\pm$  5 % and a 12 h light/dark cycle. Thirty-nine SD rats were randomly divided into plasma group, bile group, tissue (heart, liver, spleen, lung, kidney, brain) group, and urine group of EM and EG. The plasma, urine, and bile groups included three rats each, while the tissue group included nine rats. The suspensions of EM and EG (150  $\mu\text{mol/kg/d}$ , 0.5 % CMC-Na in water as a vehicle) were administered to rats for three consecutive days via oral gavages. Rats in the control group received orally administered 0.5 % CMC-Na according to some protocol. Animal welfare and experimental procedures strictly adhered to the guidelines of the Committee on the Care and Use of Laboratory Animals in China as well as related ethical regulations of Guangzhou University of Chinese Medicine.

### 2.4. Sample collection and pretreatment

For plasma collection after the last administration, 300  $\mu\text{l}$  of blood samples from orbital veins were collected at 30 min, 1, 2 and 4 h under diethyl ether anesthesia in heparinized 1.5 ml polythene tubes. The blood samples were then centrifuged at 1,057 g for 10 min. Supernatants were removed and plasma samples from the same rat at different collecting times were mixed in equal volume. For bile sample collection, rats were anesthetized by intraperitoneal injection of 25 % urethane solution. Bile samples were gathered through bile intubation from 0 to 6 h. For urine sample collection, rats were placed in metabolite cages and urine samples were collected from 0 to 24 h after the last dosing. In terms of tissue group sampling, nine rats were randomly divided into three groups with three rats for each point. Rats were executed with 10 % chloral hydrate solution by intraperitoneal injection at 1, 2, and 4 h after the last administration, respectively. Then, the rats were dissected to collect the heart, liver, spleen, lung, kidney, and brain tissues. The tissues were washed with 0.9 % saline solution and dried with filter papers. All plasma, bile, urine, and tissue samples were stored at  $-80^{\circ}\text{C}$  until analysis.

The collected plasma, bile, and urine samples were mixed with 4 times the volume of methanol to precipitate protein. The tissue samples were homogenized in an ice-bath condition with 3 times the amount (g/ml) of 0.9 % saline solution, subsequently extracted by ultrasound (power 280 W, frequency 40 kHz) for 10 min, and then centrifuged at 122, 136 g for 30 min. Supernatants were then removed, and the tissue samples from the same rat at different collection times were mixed in equal volumes. Then, the mixed supernatants added 3 times the volume of methanol, vortexed for 30 s, and then centrifuged at 122, 136 g for another 30 min. Finally, an aliquot of separate supernatants measuring 5  $\mu\text{l}$  was injected into the UHPLC-Q Exactive-Orbitrap MS system for further analysis.

## 3. Results and discussion

The metabolism profile of EM and EG *in vivo* was evaluated systematically in this study, as shown in [Supplementary Figure](#). 190 metabolites were identified using a UHPLC-Q Exactive-Orbitrap mass system, detailed information can be found in [Supplementary Table 1](#). The metabolic pathways of rat EM and EG are not only consistent with the reported hydrolysis, hydrogenation, hydroxylation, dihydroxylation, glucuronide conjugation and sulfate conjugation, but some new metabolic pathways leading to metabolites are also analysed in this manuscript. In addition to glucuronidation and sulfation, glutamic acid, ascorbic acid, glycerol, glyceric acid, and other compounds have been

identified in this manuscript among the phase II metabolites in this manuscript as forming metabolites with EM dehydration. These compounds were first identified and represent a direction in the metabolism of the compounds.

**Mass Fragmentation Pathways of EM and EG.** In the MS spectrum, the deprotonated molecular ion of EM and EG at  $m/z$  269.0457 and 431.0979 with the chemical formula of  $C_{15}H_9O_5$  and  $C_{21}H_{19}O_{10}$  were observed at 8.49 min and 6.11 min, respectively. MS<sup>2</sup> spectra of EM (**E3**) detected ions at  $m/z$  269.0456, 241.0500, and 225.0547, which were formed by the loss of H<sub>2</sub>O and CO<sub>2</sub> from EM. And MS<sup>2</sup> spectra of EG (**E54**) detected ions at  $m/z$  431.0981, 269.0456 and 225.0547. And the characteristic ion  $m/z$  269.0457 was produced by neutral loss of C<sub>6</sub>H<sub>10</sub>O<sub>5</sub> (hexose). Interestingly, the EM group samples mostly contain EG, indicating the presence of glycosylase catalyzed reactions in rats, which is inconsistent with previous reports. Metabolites **E26-1** to **E26-6** were tentatively characterized as sulfated emodin. The [M–H]<sup>–</sup> ion at  $m/z$  349.0027 (C<sub>15</sub>H<sub>9</sub>O<sub>8</sub>S) and MS<sup>2</sup> ions at  $m/z$  349.0027 and 269.0454 (C<sub>15</sub>H<sub>9</sub>O<sub>4</sub>, 80 Da, loss of SO<sub>3</sub>) were observed in the secondary mass spectrum, suggesting that metabolites **E26-1** to **E26-6** had undergone sulfate conjugation. And emodin undergoes glucuronide conjugation in rats to give metabolites **E58-1**, **E58-2** and **E58-3**, the deprotonated molecular ion  $m/z$  445.0778 with the chemical formula of C<sub>21</sub>H<sub>17</sub>O<sub>11</sub> and observed at 5.25 min, 6.04 min, and 6.58 min, product ions at  $m/z$  445.0774 (C<sub>21</sub>H<sub>17</sub>O<sub>11</sub>) and 269.0452 (C<sub>15</sub>H<sub>9</sub>O<sub>5</sub>, –176 Da).

**Identification of Metabolites In Vivo.** Metabolites **E1-1** and **E1-2** were eluted at 6.82 min and 7.60 min with same quasi-molecular [M–H]<sup>–</sup> ion at  $m/z$  237.0553 (C<sub>15</sub>H<sub>9</sub>O<sub>3</sub>) and the product ions at  $m/z$  237.0553 (C<sub>15</sub>H<sub>9</sub>O<sub>3</sub>) and 209.0662 (C<sub>14</sub>H<sub>9</sub>O<sub>2</sub>). Both parent and fragment ions are 32 Da (2O) lower than compound **E3**. Therefore, compounds **E1-1** and **E1-2** were tentatively characterized as dideoxyemodin. Similarly, compound **E2** was characterized as deoxyemodin. Since the [M–H]<sup>–</sup> ion at  $m/z$  253.0506 (C<sub>15</sub>H<sub>9</sub>O<sub>4</sub>) and MS<sup>2</sup> ions at  $m/z$  253.0501, 225.0543 and 209.0593. Both parent and fragment ions are 16 Da (O) lower than compound **E3**.

Metabolites **E4-1** and **E4-2** exhibited retention times of 6.63 min and 6.73 min and were detected at  $m/z$  271.0614 in MS spectra, demonstrating the same chemical formula of C<sub>15</sub>H<sub>11</sub>O<sub>5</sub>. Ions at  $m/z$  271.0614, 253.0485, 227.0694 are 16 Da (O) lower than compounds **E9**. Therefore, metabolites **E4-1** and **E4-2** were tentatively characterized as ring open-hehydroxyemodin. Metabolites **E9-1**, **E9-2** and **E9-3** were detected at 5.54 min, 7.76 min, and 7.90 min, with the same quasi-molecular ion [M–H]<sup>–</sup> at  $m/z$  287.0560 and an element composition of C<sub>15</sub>H<sub>11</sub>O<sub>6</sub>. MS<sup>2</sup> fragment ions at  $m/z$  269.0449 (C<sub>15</sub>H<sub>9</sub>O<sub>5</sub>), 259.0604 (C<sub>14</sub>H<sub>11</sub>O<sub>5</sub>), 243.0664 (C<sub>14</sub>H<sub>11</sub>O<sub>4</sub>), and 225.0557 (C<sub>14</sub>H<sub>9</sub>O<sub>3</sub>). From the saturation of the molecular formula and the fragment ion situation, it should be the ring opening between C9–C11 or C9–C12 of emodin, indicating that metabolites **E9-1**, **E9-2**, and **E9-3** have been tentatively characterized as ring opening emodin.

Metabolite **E5**, with an elution time at 6.72 min, showing an [M–H]<sup>–</sup> ion at  $m/z$  281.0563, indicating an element composition of C<sub>16</sub>H<sub>9</sub>O<sub>5</sub>. Ions at  $m/z$  281.0463, 253.0507, and 225.0549 were observed in the secondary mass spectrum, both parent and fragment ions are 28 Da (CO) higher than compound **E2**. Therefore, metabolite **E5** was tentatively characterized as deoxyformylated emodin.

Metabolite **E6** was eluted at 7.61 min, with the molecular formula C<sub>15</sub>H<sub>7</sub>O<sub>6</sub> at  $m/z$  283.0249. fragment ions at  $m/z$  283.0262 (C<sub>15</sub>H<sub>7</sub>O<sub>6</sub>), 255.0299 (C<sub>14</sub>H<sub>7</sub>O<sub>5</sub>), and 239.0343 (C<sub>14</sub>H<sub>7</sub>O<sub>4</sub>). Ion  $m/z$  239.0343 was formed by loss of CO<sub>2</sub> from the parent ion. Comparison with reference standard, metabolite **E6** was characterized as rhein.

Metabolites **E7-1**, **E7-2**, and **E7-3** were detected at 7.46 min, 7.59 min, and 7.66 min, with the same quasi-molecular ion [M–H]<sup>–</sup> at  $m/z$  283.0607 and giving element composition of C<sub>16</sub>H<sub>11</sub>O<sub>5</sub>. MS<sup>2</sup> ions at  $m/z$  268.0376 (C<sub>15</sub>H<sub>8</sub>O<sub>5</sub>) and 240.0422 (C<sub>14</sub>H<sub>8</sub>O<sub>4</sub>) by successive losses of CH<sub>3</sub> and CO. Metabolites **E7-1**, **E7-2** and **E7-3** were tentatively characterized as methylemodin.

Metabolites **E8-1** to **E8-8** were eluted at 5.86 min, 6.18 min, 6.68

min, 6.91 min, 7.40 min, 7.48 min, 8.78 min, and 9.01 min, showed [M–H]<sup>–</sup> ion at  $m/z$  285.0501, indicating an element composition of C<sub>15</sub>H<sub>9</sub>O<sub>5</sub>. ions at  $m/z$  285.0405, 257.0453, 241.0499, 226.0261, 213.0546, and 198.0309 were observed in the secondary mass spectrum, both parent and fragment ions are 16 Da (O) higher than compound **E3**. Therefore, metabolites **E8-1** to **E8-8** were tentatively characterized as hydroxyemodin. Metabolites **E13-1**, **E13-2**, and **E13-3** were tentatively characterized as dihydroxyemodin. The [M–H]<sup>–</sup> ion at  $m/z$  301.0356 (C<sub>15</sub>H<sub>9</sub>O<sub>7</sub>) and MS<sup>2</sup> ions at  $m/z$  301.0378, 283.0251, 273.0405, and 225.0297. fragment ions are 16 Da (O) higher than compounds **E8**. Similarly, metabolites **E17-1** and **E17-2** were tentatively characterized as dihydroxymethylemodin, since the [M–H]<sup>–</sup> ion at  $m/z$  315.0511 (C<sub>16</sub>H<sub>11</sub>O<sub>7</sub>) and MS<sup>2</sup> ions at  $m/z$  315.0511, 300.0275, 272.0372, and 244.0372. Fragment ions are 14 Da (CH<sub>2</sub>) higher than compounds **E13**. Metabolite **E40** was eluted at 6.03 min, with molecular formula C<sub>16</sub>H<sub>11</sub>O<sub>10</sub>S at  $m/z$  395.0081. fragment ions at  $m/z$  395.0081, 315.0510, 300.0277, and 272.0332, which suggested that **E40** was obtained by sulfate conjugation and dihydroxymethylemodin. Therefore, metabolite **E40** was tentatively characterized as sulfated dihydroxymethyl emodin. Metabolites **E20-1** to **E20-4** were detected at 6.28 min, 6.55 min, 6.99 min, and 7.72 min, possessing the same ion [M–H]<sup>–</sup> at  $m/z$  329.0304 and giving element composition of C<sub>16</sub>H<sub>9</sub>O<sub>9</sub>. MS<sup>2</sup> fragment ions at  $m/z$  329.0305 (C<sub>16</sub>H<sub>9</sub>O<sub>8</sub>) and 285.0404 (C<sub>15</sub>H<sub>9</sub>O<sub>6</sub>, hydroxyemodin, –CO<sub>2</sub>). Thus, metabolites **E20-1** to **E20-4** were tentatively characterized as carboxyl hydroxyemodin.

Metabolites **E10-1** and **E10-2** exhibited retention times of 6.95 min and 7.48 min and were detected at  $m/z$  297.0407 in MS spectra, showing the same chemical formula of C<sub>16</sub>H<sub>9</sub>O<sub>6</sub>. Ions at  $m/z$  297.0407, 269.0457, 225.0556 are 28 Da (CO) higher than compounds **E3**, loss of CO obtained EM, indicated that metabolites were obtained by the formylation reaction of EM. Therefore, metabolites **E10-1** and **E10-2** were tentatively characterized as formyl emodin.

Metabolite **E11** was eluted at 7.05 min, with molecular formula C<sub>15</sub>H<sub>7</sub>O<sub>7</sub> at  $m/z$  299.0201, fragment ions at  $m/z$  299.0193 (C<sub>15</sub>H<sub>7</sub>O<sub>7</sub>), 255.0299 (C<sub>14</sub>H<sub>7</sub>O<sub>5</sub>), and 227.0340 (C<sub>13</sub>H<sub>7</sub>O<sub>4</sub>). Both parent and fragment ions are 16 Da (O) higher than compound **E6**. Therefore, metabolite **E11** was tentatively characterized as emodic acid.

Metabolite **E12**, eluted with a retention time of 8.62 min, was found in MS spectra at  $m/z$  299.0552, with the molecular formula of C<sub>16</sub>H<sub>11</sub>O<sub>6</sub>, fragment ions at  $m/z$  299.0548 (C<sub>16</sub>H<sub>11</sub>O<sub>6</sub>), 284.0320 (C<sub>15</sub>H<sub>8</sub>O<sub>6</sub>), and 256.0374 (C<sub>14</sub>H<sub>8</sub>O<sub>5</sub>). Both parent and fragment ions are 16 Da (O) higher than compounds **E7**. metabolite **E12** was tentatively characterized as fallacinol. And metabolites **E36-1** to **E36-4** showed the same [M–H]<sup>–</sup> ion at  $m/z$  379.0133 (C<sub>16</sub>H<sub>11</sub>O<sub>10</sub>S) at 5.27 min, 5.90 min, 7.19 min, and 7.97 min, and MS<sup>2</sup> spectra gave ions at  $m/z$  299.0555 and 256.0377, indicating that fallacinol undergo sulfate conjugation. Thus, metabolites **E36-1** to **E36-4** were identified as sulfated fallacinol.

Metabolites **E14-1**, **E14-2**, and **E14-3** were detected at 7.85 min, 8.02 min, and 8.14 min, with the same ion [M–H]<sup>–</sup> at  $m/z$  311.0565 and an element composition of C<sub>17</sub>H<sub>11</sub>O<sub>6</sub>. MS<sup>2</sup> fragment ions at  $m/z$  311.0565 (C<sub>17</sub>H<sub>11</sub>O<sub>6</sub>), 283.0614 (C<sub>16</sub>H<sub>11</sub>O<sub>5</sub>), 269.0449 (C<sub>15</sub>H<sub>9</sub>O<sub>5</sub>), and 225.0557 (C<sub>14</sub>H<sub>9</sub>O<sub>3</sub>). The ion at  $m/z$  269.0449 was formed by the loss of C<sub>2</sub>H<sub>2</sub>O from the parent ion, so the substituent is CH<sub>3</sub>COOH. Metabolites **E14-1**, **E14-2**, and **E14-3** were tentatively characterized as acetyl emodin.

Metabolites **E15-1**, **E15-2**, and **E15-3** showed the same [M–H]<sup>–</sup> ion at  $m/z$  313.0352 (C<sub>16</sub>H<sub>9</sub>O<sub>7</sub>) at 7.75 min, 7.95 min, and 8.23 min. MS<sup>2</sup> spectra gave ions at  $m/z$  313.0352, 285.0404, and 269.0456. Fragment ion display loss of CO<sub>2</sub> gave ion  $m/z$  269.0456 (EM). Therefore, metabolites **E15-1**, **E15-2**, and **E15-3** were identified as carboxyl emodin. And metabolites **E40-1**, **E40-2**, and **E40-3** showed the same [M–H]<sup>–</sup> ion at  $m/z$  392.9930 (C<sub>16</sub>H<sub>9</sub>O<sub>10</sub>S) at 5.54 min, 5.76 min, and 7.75 min, and the MS<sup>2</sup> spectra gave ions at  $m/z$  392.9916, 313.0351, 284.0411, and 269.0456, indicating that carboxyl emodin undergo sulfate conjugation. Thus, metabolites **E40-1**, **E40-2**, and **E40-3** were identified as carboxyl-sulfated emodin.

Metabolites **E16-1** to **E16-6** were eluted at 5.17 min, 6.86 min, 7.33 min, 7.47 min, 7.62 min, and 7.93 min, showed an  $[M-H]^-$  ion at  $m/z$  313.0719 and an element composition of  $C_{17}H_{13}O_6$ . Fragment ions at  $m/z$  313.0709, 295.0608, 283.0611, and 269.0454 were observed by successive losses of  $H_2O$ ,  $CH_2O$  and  $C_2H_4O$ . Therefore, metabolites **E16-1** to **E16-6** were tentatively characterized as ethylene glycol emodin. Ethylene glycol emodin also undergo sulfate conjugation, giving the ion  $[M-H]^-$  at  $m/z$  393.0293 and an element composition of  $C_{17}H_{12}O_9S$ .  $MS^2$  fragment ions at  $m/z$  393.0293, 313.0709, 295.0612, and 269.0453. Therefore, metabolites **E41-1**, **E41-2**, and **E41-3** were tentatively characterized as ethylene glycol sulfated emodin. The proposal fragmentation pathway is shown in Fig. 2.

Metabolites **E18-1** and **E18-2** exhibited retention times of 8.35 min and 8.83 min and were detected at  $m/z$  325.0722 in the MS spectra, showing the same chemical formula of  $C_{18}H_{13}O_6$ . The ions at  $m/z$  325.0711, 283.0610, 254.0610, and 240.0426 are 42 Da ( $C_2H_2O$ ) lower than compounds **E7**. Therefore, metabolites **E18-1** and **E18-2** were tentatively characterized as methylacetylemodin. Sulfate conjugation then occurred to give metabolite **E45**, eluted with a retention time of 8.62 min, which was found in MS spectra at  $m/z$  405.0277, which is consistent with the theoretical molecular formula of  $C_{18}H_{13}O_9S$ . The fragment ions at  $m/z$  405.0269, 325.0704, 283.0597, and 254.0576.

Metabolites **E19-1**, **E19-2**, and **E19-3** were detected at 5.13 min, 7.58 min, and 7.93 min with the same ion  $[M-H]^-$  at  $m/z$  327.0517, giving element composition of  $C_{17}H_{11}O_7$ .  $MS^2$  fragment ions at  $m/z$  327.0517 ( $C_{17}H_{11}O_7$ ), 283.0614 ( $C_{16}H_{11}O_5$ ), 255.0660 ( $C_{15}H_9O_4$ ), and 239.0709 ( $C_{15}H_9O_3$ ). Removal of one molecule of  $CO_2$  to obtain 283.0614 (methylation), metabolites **E19-1**, **E19-2**, and **E19-3** were tentatively characterized as methylcarboxylemodin. Similarly, metabolite **E46**, which may undergo sulfate conjugation, was characterized as methyl sulfated carboxylemodin. Since the  $[M-H]^-$  ion at  $m/z$  407.0084 ( $C_{17}H_{11}O_{10}S$ ) and  $MS^2$  ions at  $m/z$  327.0508, 283.0615, 255.0662, and 239.0708.

Metabolites **E21-1** and **E21-2** exhibited retention times of 6.02 min and 6.72 min and were detected at  $m/z$  333.0076 in the MS spectra, showing the same chemical formula of  $C_{15}H_9O_7S$ . Ions at  $m/z$  333.0066 and 253.0504 ( $C_{15}H_9O_4$ , 80 Da, loss of  $SO_3$ ) were observed in the secondary mass spectrum, suggesting that metabolites **E21-1** and **E21-2** had undergone sulfate conjugation, and were tentatively characterized as sulfated deoxyemodin. Metabolites **E31-1**, **E31-2**, and **E31-3** were characterized as sulfated methylemodin. The  $[M-H]^-$  ion at  $m/z$  363.0174 ( $C_{16}H_{11}O_8S$ ) and the  $MS^2$  ions at  $m/z$  363.0174, 283.0605, and 240.0418. Similarly, metabolites **E32-1** to **E32-6** were characterized as sulfated hydroxyemodin. The  $[M-H]^-$  ion at  $m/z$  364.9972 ( $C_{15}H_9O_9S$ ) and the  $MS^2$  ions at  $m/z$  285.0403 and 241.0500. metabolites **E35-1** and **E35-2** were characterized as sulfated emodic acid. Since  $[M-H]^-$  ion at  $m/z$  378.9758 ( $C_{16}H_9O_9S$ ) and  $MS^2$  ions at  $m/z$  378.9758 and 299.0194.

Metabolite **E22**, eluted with a retention time of 8.01 min, was found in MS spectra at  $m/z$  339.0511, consistent with the theoretical molecular formula of  $C_{18}H_{11}O_7$ .  $MS^2$  fragment ions at  $m/z$  399.0503 ( $C_{18}H_{11}O_7$ ), 311.0556 ( $C_{17}H_{11}O_6$ ), 269.0453 ( $C_{15}H_9O_5$ ), 241.0500 ( $C_{14}H_6O_4$ ), and 225.0547 ( $C_{14}H_9O_3$ ). Ion  $m/z$  269.0453 was obtained by continuous loss of CO and COCH<sub>3</sub>. Therefore, metabolite **E22** was tentatively characterized as formyl acetyl emodin.

Metabolites **E23-1**, **E23-2**, and **E23-3** were detected at 6.98 min, 7.58 min, and 7.86 min, respectively, with the same ion  $[M-H]^-$  at  $m/z$  341.0667 and an element composition of  $C_{18}H_{13}O_7$ .  $MS^2$  fragment ions at  $m/z$  341.0667 ( $C_{18}H_{13}O_7$ ), 323.0554 ( $C_{18}H_{11}O_6$ ), 308.0328 ( $C_{17}H_8O_6$ ), 295.0612 ( $C_{17}H_{11}O_5$ ), 283.0614 ( $C_{16}H_{11}O_5$ ), and 269.0453 ( $C_{15}H_9O_5$ ). The compound shows an additional molecule of  $C_3H_6O_3$  compared to EM, possibly lactic acid. Based on the literature and fragment ions, metabolites **E23-1**, **E23-2**, and **E23-3** were tentatively characterized as lactated emodin. Similarly, metabolites **E25-1** to **E25-4** were tentatively characterized as glycerol emodin. Since  $[M-H]^-$  ion at  $m/z$  343.0463 ( $C_{17}H_{11}O_8$ ) and  $MS^2$  ions at  $m/z$  343.0817, 325.0711,

283.0612, and 269.0465. Fragment ions are 2 Da ( $H_2$ ) higher than compounds **E23**. Thus, metabolite **E50** and **E51** were detected at 4.24 min and 5.07 min, showing  $[M-H]^-$  ions at  $m/z$  421.0245 ( $C_{18}H_{13}O_{10}S$ ) and 423.0033 ( $C_{17}H_{11}O_{11}S$ ).  $MS^2$  of **E50** fragment ions at  $m/z$  341.0667 ( $C_{18}H_{13}O_7$ , -80 Da, loss of  $SO_3$ ), 323.0554, 308.0328, 295.0612, 281.0456, and 269.0453. And  $MS^2$  of **E51** fragment ions at  $m/z$  343.0453 ( $C_{17}H_{11}O_8$ , -80 Da, loss of  $SO_3$ ), 325.0351, 299.0559, 281.0457, and 269.0465. Therefore, metabolite **E50** was characterized as sulfated lactated emodin and **E51** was characterized as sulfated carboxyl fallacinal.

Metabolites **E24-1** and **E24-2** exhibited retention times of 6.32 min and 6.75 min and were detected at  $m/z$  343.0463 in MS spectra, showing the same chemical formula of  $C_{17}H_{11}O_8$ . The  $MS^2$  ions at  $m/z$  343.0470, 299.0561, 281.0458, and 253.0505, which were 44 Da (COOH) higher than compound **E12**. Therefore, metabolites **E24-1** and **E24-2** were tentatively characterized as carboxyl fallacinal.

Metabolites **E27-1**, **E27-2**, and **E27-3** were detected at 6.54 min, 7.19 min, and 7.95 min, with the same ion  $[M-H]^-$  at  $m/z$  355.0463 and an element composition of  $C_{18}H_{11}O_8$ .  $MS^2$  fragment ions at  $m/z$  355.0455 ( $C_{18}H_{11}O_8$ ), 327.0507 ( $C_{17}H_{11}O_7$ ), 311.0573 ( $C_{17}H_{11}O_6$ ), 296.0325 ( $C_{16}H_8O_6$ ), 283.0611 ( $C_{16}H_{11}O_5$ ), 269.0453 ( $C_{15}H_9O_5$ ), and 240.0426 ( $C_{14}H_8O_4$ ). The compound shows an additional molecule of  $C_3H_4O_4$  compared to EM, possibly malic acid. According to the literature, metabolites **E27-1**, **E27-2**, and **E27-3** were tentatively characterized as malonyl emodin.

Metabolites **E28-1** to **E28-4** were eluted at 7.50 min, 7.81 min, 7.98 min, and 8.10 min and showed an  $[M-H]^-$  ion at  $m/z$  355.0815, indicating an element composition of  $C_{19}H_{15}O_7$ . Fragment ions were observed at  $m/z$  355.0806, 237.0696, 325.0702, 307.0600, 282.0523, and 269.0450. The compound shows an additional molecule of  $C_4H_8O_3$  compared to EM, possibly hydroxybutyric acid. Therefore, metabolites **E28-1** to **E28-4** were tentatively characterized as hydroxybutyryl emodin.

Metabolites **E29-1** ( $R_t = 6.27$  min) and **E29-2** ( $R_t = 6.48$  min) showed the same  $[M-H]^-$  ion at  $m/z$  357.0258 ( $C_{17}H_9O_9$ ) and  $MS^2$  spectra gave ions at  $m/z$  313.0352 ( $C_{16}H_9O_7$ , - $CO_2$ ), 269.0457 ( $C_{15}H_9O_5$ , - $CO_2$ ), 241.0503 ( $C_{14}H_9O_4$ ), and 225.0547 ( $C_{14}H_9O_3$ ). Fragment ions  $m/z$  269.0457, 241.0503, and 225.0547 were the same as the fragment ion of EM, and ion  $m/z$  269.0457 was obtained by two consecutive losses of  $CO_2$ , metabolites **E29-1** and **E29-2** were identified as dicarboxyl emodin.

Metabolites **E30-1** to **E30-4** were eluted at 6.02 min, 6.80 min, 7.21 min, and 7.89 min, showing an  $[M-H]^-$  ion at  $m/z$  357.0611, indicating an element composition of  $C_{18}H_{13}O_8$ . Fragment ions were observed at  $m/z$  357.0603, 313.0704, 295.0600, 283.0603, and 269.0450. The compound exhibits an additional molecule of  $C_3H_6O_4$  compared to EM, possibly glyceric acid. Therefore, metabolites **E30-1** to **E30-4** were tentatively characterized as glyceric acid emodin.

Metabolites **E33-1** and **E33-2** exhibited retention times of 7.81 min and 7.64 min and were detected at  $m/z$  369.0985 in MS spectra, showing the same chemical formula of  $C_{20}H_{17}O_7$ . Fragment ions at  $m/z$  369.0977, 315.0875, 325.0715, 283.0612, and 269.0457. The compound shows an additional molecule of  $C_5H_{10}O_3$  compared to EM, possibly hydroxyvaleric acid, were tentatively characterized as hydroxyvaleryl emodin. Similarly, metabolites **E34-1** and **E34-2** were characterized as erythrose emodin. Since  $[M-H]^-$  ion at  $m/z$  371.0767 ( $C_{19}H_{15}O_8$ ) and  $MS^2$  ions at  $m/z$  371.0757, 353.0658, 341.0650, 323.0556, 311.0550, 295.0603, 283.0609, 269.0447, and 225.0542. The compound shows an additional molecule of  $C_4H_8O_4$  compared to EM, possibly erythrose. The proposal fragmentation pathway is shown in Fig. 1.

Metabolites **E37-1**, **E37-2**, and **E37-3** exhibited retention times of 4.97 min, 5.16 min, and 5.34 min and were detected at  $m/z$  380.9924 in MS spectra, indicating the same chemical formula of  $C_{15}H_9O_{10}S$ . Fragment ions at  $m/z$  380.9906 and 301.0351 ( $C_{15}H_9O_7$ , -80 Da, loss of  $SO_3$ ) were observed in the secondary mass spectrum, suggesting that

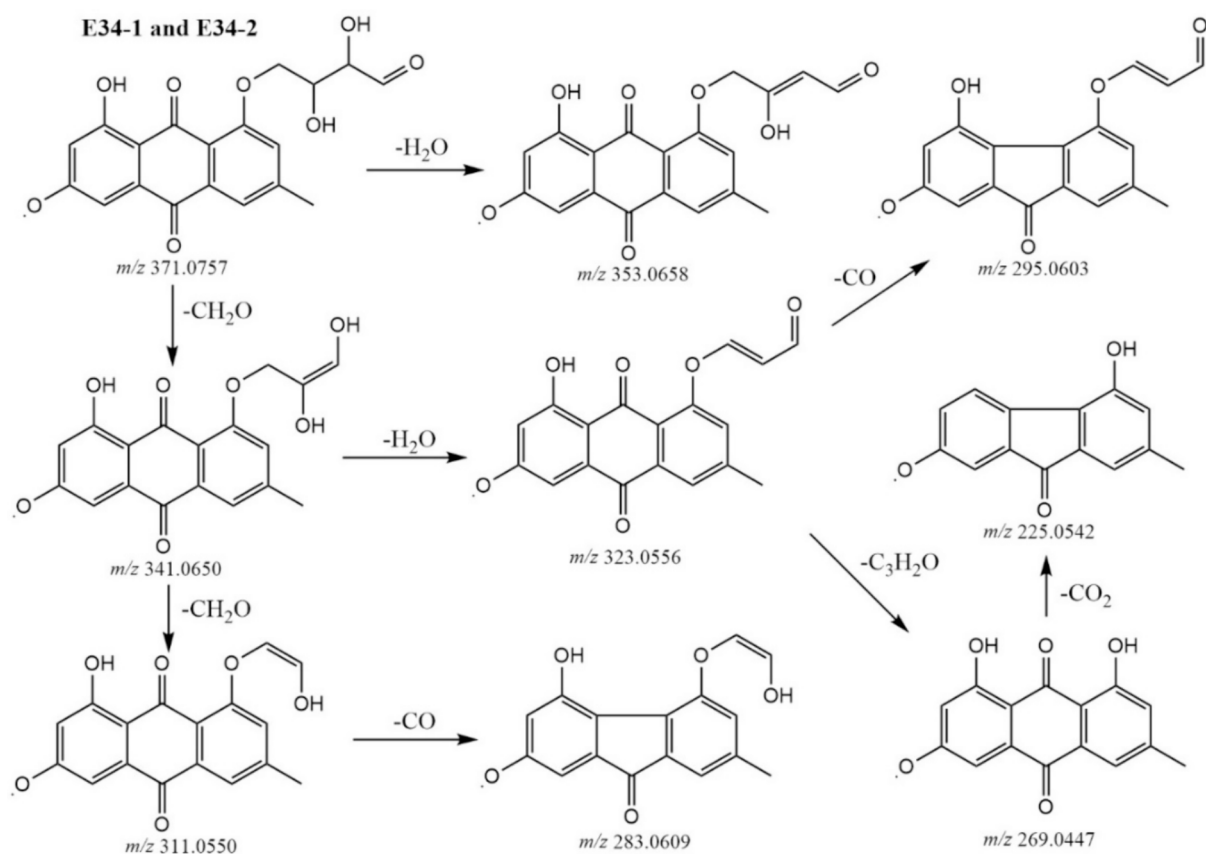


Fig. 1. The proposal fragmentation pathways of compounds E34-1 and E34-2.

metabolites **E37-1**, **E37-2**, and **E37-3** had undergone sulfate conjugation. Therefore, they were tentatively characterized as sulfated dihydroxyemodin.

Metabolites **E38-1**, **E38-2**, and **E38-3** showed the same  $[M-H]^-$  ion at  $m/z$  383.0778 ( $C_{20}H_{15}O_8$ ) and detected at 7.28 min, 7.66 min, and 7.94 min, and  $MS^2$  spectra gave ions at  $m/z$  383.0765, 339.0869, 321.0762, 296.0689, 281.0453, and 269.0463. The compound shows an additional molecule of  $C_5H_8O_4$  compared to EM, possibly glutaryl. Thus, metabolites **E38-1**, **E38-2**, and **E38-3** were characterized as glutaryl emodin. Similarly, metabolites **E39-1**, **E39-2**, and **E39-3** were characterized as hydroxybenzoyl emodin. The  $[M-H]^-$  ion at  $m/z$  389.0660 ( $C_{22}H_{13}O_7$ ) and the  $MS^2$  ions at  $m/z$  389.0660 and 269.0459.

Metabolites **E43-1**, **E43-2**, and **E43-3** were detected at 5.41 min, 5.98 min, and 7.04 min, respectively, with the same ion  $[M-H]^-$  at  $m/z$  398.0884 and an element composition of  $C_{20}H_{16}O_8N$ .  $MS^2$  fragment ions at  $m/z$  398.0870 ( $C_{20}H_{16}O_8N$ ), 381.0611 ( $C_{20}H_{13}O_8$ ), 354.0978 ( $C_{19}H_{16}O_6N$ ), 337.0708 ( $C_{19}H_{13}O_6$ ), 325.0724 ( $C_{18}H_{13}O_6$ ), 311.0558 ( $C_{17}H_{11}O_6$ ), 298.0723 ( $C_{16}H_{12}O_5N$ ), 283.0613 ( $C_{16}H_{11}O_5$ ), and 269.0453 ( $C_{15}H_9O_5$ ). The compound has an additional molecule of  $C_5H_9O_4N$  compared to EM, possibly glutamic acid. According to literature and fragment ions. Metabolites **E43-1**, **E43-2**, and **E43-3** were tentatively characterized as glutamyl emodin. Similarly, metabolites **E44-1**, **E44-2**, and **E44-3** were characterized as hydroxyglutaryl emodin. Since the  $[M-H]^-$  ion at  $m/z$  399.0726 ( $C_{20}H_{15}O_9$ ) and  $MS^2$  ions at  $m/z$  399.0717, 355.0823, 311.0919, 283.0610, and 269.0459. The compound shows an additional molecule of  $C_5H_8O_5$  compared to EM, possibly hydroxyglutaric acid.

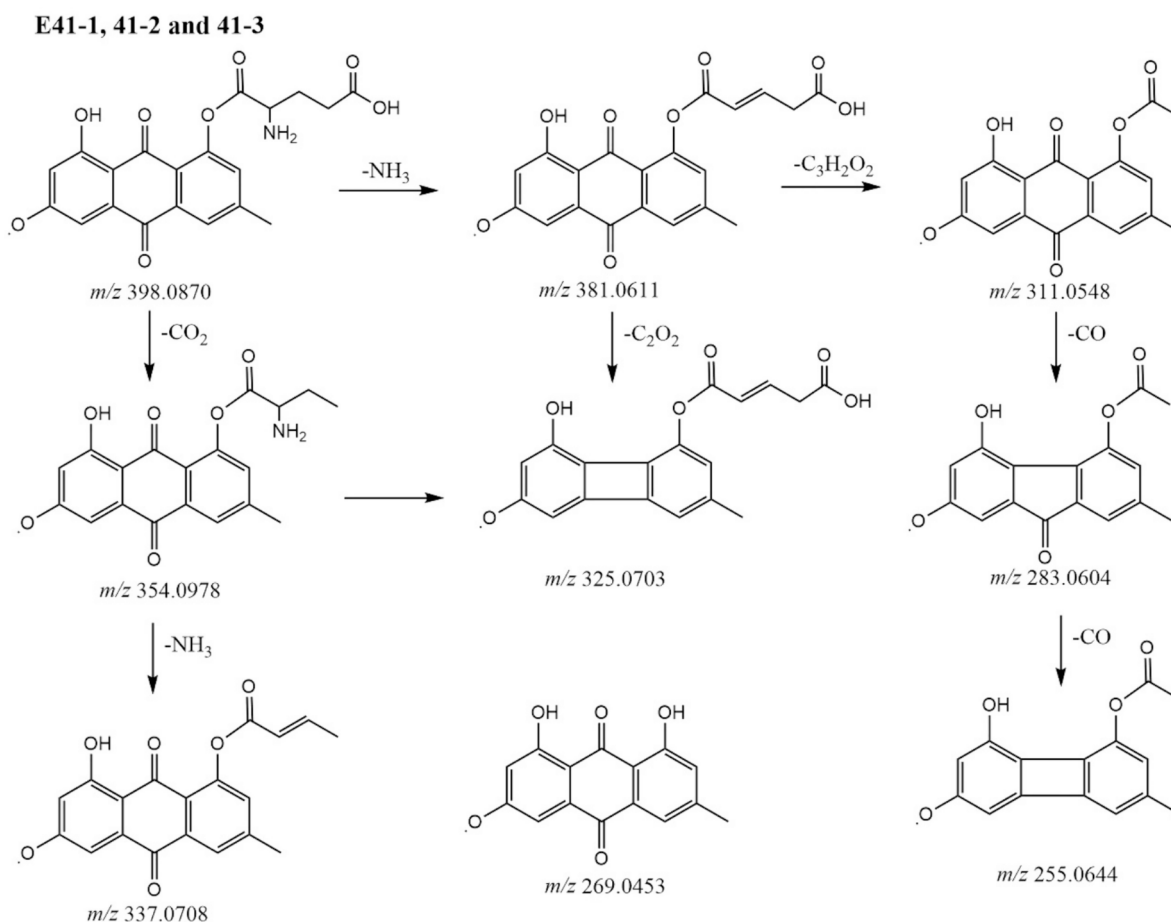
Metabolites **E47-1**, **E47-2**, and **E47-3** showed retention times of 4.92 min, 5.28 min, and 6.19 min and were detected at  $m/z$  408.9875 in MS spectra, showing the same chemical formula of  $C_{16}H_9O_{11}S$ . Fragment ions at  $m/z$  408.9875, 329.0309 ( $C_{19}H_9O_8$ ,  $-80$  Da, loss of  $SO_3$ ), 314.0067, and 286.0124 were observed in the secondary mass

spectrum, suggesting that metabolites **E37-1**, **E37-2**, and **E37-3** were obtained by sulfate conjugation with metabolites **E20**. Therefore, metabolites **E37-1**, **E37-2**, and **E37-3** were tentatively characterized as sulfated carboxyl hydroxyemodin.

Metabolite **E48** was eluted at 7.16 min, with molecular formula  $C_{20}H_{13}O_8N_2$  at  $m/z$  409.0686. The fragment ions at  $m/z$  409.0675 ( $C_{20}H_{13}O_8N_2$ ), 329.0291 ( $C_{16}H_9O_8$ ), and 269.0457 ( $C_{15}H_9O_5$ ). The compound shows an additional molecule of  $C_5H_6O_4N_2$  compared to EM, which may be dihydroorotic acid, but this is uncertain and is provisionally defined as unknown. The metabolites **E49-1** and **E49-2** were also unknown.  $[M-H]^-$  ion at  $m/z$  416.0777 ( $C_{23}H_{14}O_7N$ ) and  $MS^2$  ions at  $m/z$  398.0674, 370.0728, 354.0769, 326.0817, and 269.0459. And metabolite **E57** was unknown,  $[M-H]^-$  ion at  $m/z$  437.0993 ( $C_{22}H_{17}O_8N_2$ ) and  $MS^2$  ions at  $m/z$  437.0994, 419.0883, 376.0822, 358.0715, and 269.0457.

Metabolites **E52-1** ( $R_t = 6.69$  min) and **E52-2** ( $R_t = 6.96$  min) showed the same  $[M-H]^-$  ion at  $m/z$  427.0673 ( $C_{21}H_{15}O_{10}$ ) and  $MS^2$  spectra gave ions at  $m/z$  427.0673 ( $C_{21}H_{15}O_{10}$ ) and 269.0455 ( $C_{15}H_9O_5$ ). The compound shows an additional molecule of  $C_6H_8O_6$  compared to EM, possibly ascorbic acid (VC). Therefore, metabolites **E52-1** and **E52-2** were identified as ascorbyl emodin.

Metabolites **E53-1** to **E53-4** were eluted at 6.16 min, 6.28 min, 6.83 min, and 7.31 min and showed an  $[M-H]^-$  ion at  $m/z$  429.0835 with an element composition of  $C_{21}H_{17}O_{10}$ . The fragment ion of **E53-1** to **E53-3** at  $m/z$  253.0505 ( $C_{15}H_9O_4$ ), which was obtained by the loss of  $C_6H_8O_6$  (176 Da), indicated that they undergo glucuronide conjugation. Therefore, metabolites **E53-1** to **E53-3** were characterized as glucuronide deoxyemodin. The  $MS^2$  spectra of **E53-4** gave ions at  $m/z$  429.0820, 411.0675, 401.0883, 383.0770, 351.0511, 311.0557, and 269.0455. The compound shows an additional molecule of  $C_6H_{10}O_6$  compared to EM, possibly glucosone. Thus, metabolite **E53-4** was tentatively characterized as glucosone emodin.



Metabolite **E55**, eluted with a retention time of 7.57 min, was found in the MS spectra at  $m/z$  434.0872, which is consistent with the theoretical molecular formula of  $C_{23}H_{16}O_8N$ . The fragment ions at  $m/z$  434.0866, 416.0754, 389.1027, 372.0863, 354.0757, 325.0343, 308.0316, 297.0394, 281.0448, and 269.0449 were observed. The compound shows an additional molecule of  $C_8H_9O_4N$  compared to EM and possibly dihydroxyphenylglycine. Thus, metabolite **E55** was tentatively characterized as dihydroxyphenylglycine emodin. Similarly, metabolites **E61-1** and **E62-2** were identified as trihydroxyphenylglycine emodin with the  $[M-H]^-$  ion at  $m/z$  450.0823 ( $C_{23}H_{16}O_9N$ ) and  $MS^2$  ions at  $m/z$  450.0818, 432.0702, 405.0976, 388.0803, 370.0692, 325.0345, 297.0396, 281.0488, and 269.0458. Both parent and fragment ions are 16 Da (O) higher than compound **E55**. Additionally, the metabolite **E64** was identified as dihydroxy-methoxyphenylglycine emodin with the  $[M-H]^-$  ion at  $m/z$  464.0974 ( $C_{24}H_{18}O_9N$ ) and the  $MS^2$  ions at  $m/z$  464.0970, 446.0861, 418.0933, 402.0989, 384.0879, 370.0692, 325.0345, 297.0396, 281.0488, and 269.0458. Both parent and fragment ions are 14 Da ( $CH_2$ ) higher than metabolites **E61**.

Metabolite **E57**, with an elution time of 6.04 min, showed  $[M-H]^-$  ion at  $m/z$  441.0944, indicating an element composition of  $C_{21}H_{17}O_9N_2$ . Fragment ions at  $m/z$  441.0941, 296.0565, and 269.0457 were observed in the secondary mass spectrum. The compound shows an additional molecule of  $C_6H_{10}O_5N_2$  compared to EM, possibly N-carbamyl-L-glutamic acid. Therefore, metabolite **E57** was tentatively characterized as N-carbamyl-L-glutamyl emodin.

Metabolites **E59-1** ( $R_t = 5.12$  min) and **E59-2** ( $R_t = 5.47$  min) showed the same  $[M-H]^-$  ion at  $m/z$  447.0933 ( $C_{21}H_{19}O_{11}$ ) and  $MS^2$  spectra gave ions at  $m/z$  447.0930 ( $C_{21}H_{19}O_{11}$ ), 285.0401 ( $C_{15}H_9O_6$ ,  $-C_6H_{10}O_5$ ), 268.0378 ( $C_{15}H_8O_6$ ), and 241.0499 ( $C_{14}H_9O_4$ ). Metabolites **E59-1** and **E59-2** were identified as hydroxyemodin-O-glucoside.

Similarly, metabolites **E60-1**, **E60-2**, and **E60-3** were identified as open ring emodin-O-glucoside. The  $[M-H]^-$  ion at  $m/z$  449.1093 ( $C_{21}H_{21}O_{11}$ ) and  $MS^2$  ions at  $m/z$  449.1086, 431.0978, 269.0456, and 254.0583. Fragment ions indicated that the metabolites lose  $H_2O$  to give 431.0978 (EG), and lose glycosides to give ion 269.0457 (EM). And, metabolite **E69** was tentatively characterized as sulfated hydroxyemodin-O-glucoside. Since  $[M-H]^-$  ion at  $m/z$  527.0504 ( $C_{21}H_{19}O_{14}S$ ) and  $MS^2$  ions at  $m/z$  447.0933 ( $C_{21}H_{19}O_{11}$ ,  $-80$  Da) and 285.0404.

Metabolites **E62-1** to **E62-4**, eluted at retention times of 6.31 min, 6.52 min, 6.62 min, and 6.99 min, were found in MS spectra at  $m/z$  459.0937, which is consistent with the theoretical molecular formulae of  $C_{22}H_{19}O_{11}$ . Fragment ions at  $m/z$  283.0614 ( $C_{16}H_{11}O_5$ ) due to loss of  $C_6H_8O_6$  ( $-176$  Da), suggested that the metabolites undergo glucuronide conjugation. Thus, metabolites **E62-1** to **E62-4** were tentatively characterized as methylemodin-O-glucuronide. Similarly, metabolites **E63-1** to **E63-6** were characterized as hydroxyemodin-O-glucuronide. Since The  $[M-H]^-$  ion at  $m/z$  461.0728 ( $C_{21}H_{17}O_{12}$ ) and the  $MS^2$  ion at  $m/z$  285.0403 ( $C_{15}H_9O_6$ ) were determined by loss of  $C_6H_8O_6$  ( $-176$  Da). And metabolites **E65-1** and **E65-2** were characterized as emodic acid-O-glucuronide. Since  $[M-H]^-$  ion at  $m/z$  475.0521 ( $C_{21}H_{15}O_{13}$ ) and  $MS^2$  ion at  $m/z$  299.0194. Subsequently, metabolite **E67** was characterized as methyl acetylemodin-O-glucuronide. Since  $[M-H]^-$  ion at  $m/z$  501.1040 ( $C_{24}H_{21}O_{12}$ ) and  $MS^2$  ions at  $m/z$  325.0711, 283.0609, 254.0582.

Metabolites **E66-1** ( $R_t = 3.63$  min) and **E66-2** ( $R_t = 3.86$  min) showed the same  $[M-H]^-$  ion at  $m/z$  478.0450 ( $C_{20}H_{16}O_{11}NS$ ) and  $MS^2$  spectra gave ions at  $m/z$  398.0870 ( $C_{20}H_{16}O_8N$ ,  $-80$  Da), 381.0611, 354.0978, 337.0708, 325.0724, 311.0558, 298.0723, 283.0613, 269.0456, and 225.0547. Fragment ions were identical to same as

metabolites E43. Therefore, metabolites E66-1 and E66-2 were identified as sulfated glutamyl emodin.

Metabolites E68-1 to E68-4 exhibited retention times of 4.06 min, 4.43 min, 5.02 min, and 6.81 min and were detected at  $m/z$  525.0344 in MS spectra, showing the same chemical formula of  $C_{21}H_{17}O_{14}S$ . Fragment ions at  $m/z$  445.0773 and 269.0456 were probably obtained by the successive loss of  $SO_3$  (-80 Da) and  $C_6H_8O_6$  (-176 Da) from the deprotonated molecular ion at  $m/z$  581.1500. Therefore, metabolites E68-1 to E68-4 were identified as sulfated emodin-O-glucuronide. Similarly, metabolites E70-1, E70-2, and E70-3 were characterized as sulfated hydroxyemodin-O-glucuronide. The  $[M-H]^-$  ion at  $m/z$  541.0295 ( $C_{20}H_{15}O_9$ ) and the  $MS^2$  ions at  $m/z$  541.0291, 461.0730 (-80 Da), and 285.0406 (-176 Da).

Metabolites E71-1 to E71-5 showed the same  $[M-H]^-$  ion at  $m/z$  607.1315 ( $C_{27}H_{27}O_{16}$ ) at 4.40 min, 4.58 min, 4.81 min, 5.12 min, and 5.30 min, and  $MS^2$  spectra gave ions at  $m/z$  607.1309, 445.0764, 431.0987, 269.0455, and 225.0548, probably due to the successive loss of  $C_6H_{10}O_5$  (-162 Da) and  $C_6H_8O_6$  (-176 Da) from the deprotonated molecular ion at  $m/z$  607.1309, suggesting that they undergo glucoside and glucuronide conjugation. Metabolites E71-1 to E71-5 were identified as emodin-O-glucoside-O-glucuronide.

Metabolites E72-1 to E72-4 showed the same  $[M-H]^-$  ion at  $m/z$  621.1101 ( $C_{27}H_{25}O_{17}$ ) at 3.41 min, 3.75 min, 4.36 min, and 4.82 min, and  $MS^2$  spectra gave ions at  $m/z$  621.1087, 445.0764, 269.0455, and 225.0548, which were probably obtained by the successive loss of  $C_6H_8O_6$  (-176 Da) and  $C_6H_8O_6$  (-176 Da) from the deprotonated molecular ion, indicating that they undergo di-glucuronide conjugations. Thus, metabolites E72-1 to E72-4 were identified as emodin-O-diglucuronide. Similarly, metabolites E73-1 and E73-2 were characterized as hydroxyemodin-O-diglucuronide. Since the  $[M-H]^-$  ion at  $m/z$  637.1050 ( $C_{27}H_{25}O_{18}$ ) and the  $MS^2$  ions at  $m/z$  637.1050, 461.0725, and 285.0406.

**Organizational distribution of EM and EG** A total of 190 metabolites were identified in the EM and EG groups. Detailed information can be found in [Supplementary Appendix Tabl 1](#), while the proposed metabolic pathways of EM and EG are illustrated in [Fig. 3](#). To show the distribution of the metabolites, we generate a heat map by plotting the logarithmic values of the peak areas of the metabolites in urine, blood, bile, brain, heart, liver, spleen, lung and kidney tissues to show the distribution of metabolites, heat map is shown in [Fig. 4](#). Intuitively,

urine contains the most metabolites, which is consistent with the metabolic distribution pattern. Only 3 metabolites can be detected in all samples, including EM (E3) and two types of glucuronides of emodin (E58-1 and E58-2). 57 metabolites are distributed only in urine samples, other metabolites are distributed in each sample. Clustering analysis showed that the EM and EG groups of tissue samples are clustered together, indicating a similar distribution of metabolites. Interestingly, the distribution of lung tissue in the emodin group is similar to that of brain tissue of in both groups. Kidneys and blood distributions are similar, as are heart and liver distributions. The specific situation of each organization is described below.

**Metabolites in the urine** 173 and 157 metabolites were found in the urine of the EM and EG groups. The EM group contained all types of compounds, but some isomers were not been detected. In the EG group, some isomers and 4 types of E46 (methyl sulfated carboxyl emodin), E57 (carglutamine emodin), E61 (trihydroxyphenylglycine emodin), and E66 (sulfated glutamyl emodin) were not detected, which were only found in the urine of the EM group. It is interesting to note that some metabolites were not detected in blood and urine, but were detected in samples such as heart and liver. The most likely reasons for this are that the concentration in the blood is too low to be detected and insufficient sensitivity of detection equipment, or that the metabolism is too fast and then quickly converted and used up in the heart or liver.

**Metabolites in the blood** 65 and 68 metabolites were found in the blood of the EM and EG groups. In the EM group, EM, rehin, hydroxyemodin, emodic acid, fallacinal, acetyl emodin, dihydroxymethylemodin, methyl carboxylemodin, carboxyl hydroxyemodin, glyceryl emodin, erythrose emodin, ascorbyl emodin, EG, and 41 sulfate conjugations and glucuronide conjugations were found. No acetyl emodin, ascorbyl emodin, methylemodin-O-glucuronide were found in the EG group, but methylemodin, ethylene glycol emodin, methyl-acetylemodin, formyl acetyl emodin, lactated emodin, glycol emodin, malonyl emodin, and 38 sulfate conjugates and glucuronide conjugations were detected. In theory, drugs are absorbed into the blood and then distributed to different tissues. However, a large number of metabolites were not detected in blood samples, which may be due to low sample content, insufficient sensitivity of detection equipment, and rapid elimination of metabolites ([Chen et al., 2014](#); [Sun et al., 2007](#)).

**Metabolites in the bile** 27 and 16 metabolites were found in the bile of the EM and EG groups. The EM group found deoxyemodin, EM and 3

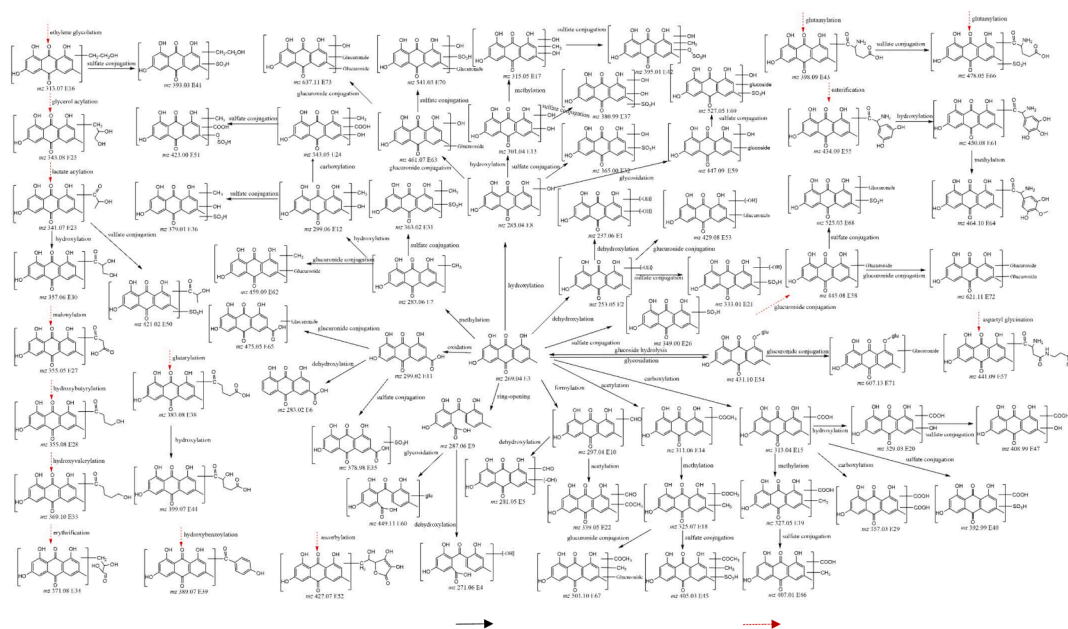


**Fig. 3.** Proposed metabolic pathways of EM and EG in rats (: React in the direction of the arrow, : Direct reaction with EM).

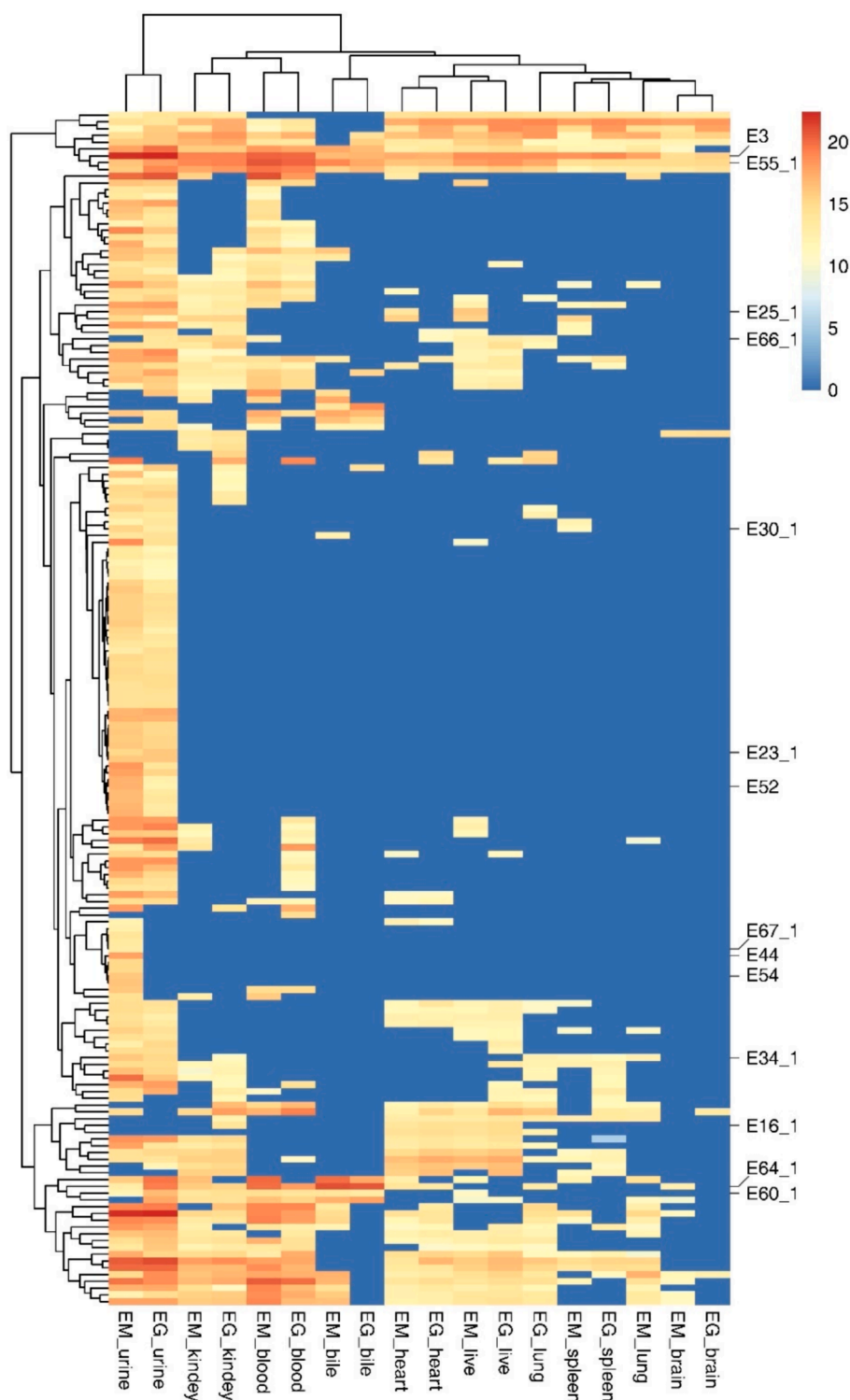


**Fig. 4.** Heat map of 190 metabolites in each organization. The yellow color in the gradient indicates an increase. The blue indicated that there are no compounds present in the sample. (X-axis: (Each sample group of EM and EG;Y-axis: 190 compounds).

hydroxymodins, and sulfate conjugates and glucuronide conjugates of several metabolites, but no EG was found, which is the only sample without EG. The EG group detected EM, EG, and sulfate conjugates and glucuronide conjugates. The metabolites in the bile are very pure, all of which are sulfate conjugates and glucuronide conjugates, suggesting that other phase II metabolites are formed in the small intestine or other tissues or enter directly into the bloodstream.

**Metabolites in the brain** 17 and 11 metabolites were found in the

brain of the EM and EG groups. The EM group found EM, EG, ethylene glycol emodin, glyceroyl emodin, erythro emodin, and sulfate conjugates and glucuronide conjugates. The EG group detected EM, EG, ethylene glycol emodin, glyceroyl emodin, erythro emodin, and glucuronide conjugations. curiously, the sulfate conjugate was not detected. It can be seen that the phase II metabolites of emodin can cross the blood–brain barrier and EM can also be hydrolysed from phase II metabolites. Interestingly, compounds such as ethylene glycol emodin,

glycoyl emodin and ether emodin can easily cross the blood–brain barrier and have high concentrations. It is speculated that they provide energy to brain tissue to improve memory.

**Metabolites in the heart** 52 and 47 metabolites were found in the heart of the EM and EG groups, respectively. In the EM group, EM, ring-opened hehydroxyemodin, rehin, methylemodin, hydroxyemodin, emodic acid, ethylene glycol emodin, dihydroxymethylemodin, glycerol emodin, glyceryl emodin, erythrose emodin, dihydroxybutanoic acid, hydroxyglutaryl emodin, ascorbyl emodin, EG, and 21 sulfate and glucuronide conjugates were found. No dihydroxymethylmodulin and dihydroxybutanoic acid were detected in the EG group, while the others were basically the same except for different amounts of isomers.

**Metabolites in the liver** 61 and 58 metabolites were found in the liver of the EM and EG groups. The EM group detected more fallacinol, dihydroxymodulin, carbonyl emodin, methylacetylemodin, methyl-carbonylemodin, and lactated emodin than the heart group. Compared to the EM group, the EG group detected acetyl emodin, formaryl acetyl emodin and no dihydroxymodulin. Components such as ethylene glycol, glycerol and glycerate, together with emodin, should undergo phase II metabolic enzymes in the liver to produce a series of metabolites which are then transported to tissues such as the heart, spleen and brain, consuming small and medium lipids in the liver which play a nutritional support role in other tissues. May be the main pathway for the treatment of fatty liver.

**Metabolites in the spleen** 32 and 27 metabolites were found in the spleen of the EM and EG groups. In the EM group, EM, hydroxyemodin, formyl emodin, emodic acid, ethylene glycol emodin, dihydroxyemodin, glycerol emodin, hydroxybutyryl emodin, glyceryl emodin, erythrose emodin, dihydroxybutanoic acid, EG, and sulfate conjugates and glucuronide conjugates. The distribution of the EG and EM groups is similar.

**Metabolites in the lung** 32 and 46 metabolites were found in the lung of the EM and EG groups. In the EM group, EM, hydroxyemodin, emodic acid, ethylene glycol emodin, glyceryl emodin, erythrose emodin, EG, and sulfate conjugates and glucuronide conjugates were found. There are 14 more metabolites distributed in the EG group than in the EM group, including: methylmodulin, acetyl emodin, acetylated fallacinol, maloyl emodin, hydroxybutyryl emodin, ascorbyl emodin. This is the reason for the performance of the EG group lung tissue in the cluster analysis. The interesting comparison is that there are metabolites such as ethylene glycol and glycerol emodin in the lung sample, but no glycerol emodin was detected.

**Metabolites in the kidney** 65 and 76 metabolites were found in the kidney of the EM and EG groups. The nature of the metabolites in the kidney sample is very similar to that in the liver sample, and there is no clustering related to the number and peak intensity of isomers. Compared with the liver metabolites, the EM group detected carbonyl hydroxyemodin, acetylated fallacinol, and hydroxybutyryl emodin, but not dihydroxyemodin and hydroxyglutaryl emodin. The EG group detected more dihydroxymodulin and acetyl emodin than the EM group of kidneys.

The heat map clearly shows that the EM and EG groups of each sample are clustered, indicating that the amount and distribution of metabolites of EM and EG in each sample are basically consistent, which supports this view. The kidney and blood samples of the EM and EG groups are clustered, while the heart and liver samples are clustered. It is curious that the lung tissue of EM is clustered with the brain tissue of EM and EG groups. This article identifies a large number of new metabolites and analyzes the distribution and characteristics of these compounds, providing a new material basis and theoretical basis for further research into the efficacy and hepatotoxicity mechanisms of EM and EG.

#### 4. Conclusion

A UHPLC-Q-Exactive MS method was established to identify and distribute of metabolites in rats following co-administration of EM and

EG by gavage. 190 metabolites were identified in rat urine, plasma, bile, heart, liver, spleen, lung, kidney, and brain. In addition to the reported hydrolysis, hydroxylation, methylation, carboxylation, glucuronidation, sulfation, etc., some new phase II metabolites have also been discovered, including formylation, acetylation, glycol acylation, lactation, glycerolisation, malonylation, glycerol acid acylation, hydroxyvalerylation, erythroxylation, glutaric acidification, hydroxybenzoylation, glutamylolation, hydroxyglutamylolation, ascorbylation, aspartyl glycylation, dihydroxyphenyl glycylation, trihydroxyphenyl glycylation, dihydroxymethoxyphenyl glycylation, and ring opening of EM, as well as their glucuronide conjugation and sulfate conjugation. Interestingly, we detected EM in all tissues and EG in all samples except bile in the EM group, indicating glycosylation of EM in rats, which differs from published research results. In the liver, EM was found to bind metabolites such as ethylene glycol, glycerol, and glycerate, which may be related to the therapeutic effect of EM on fatty liver. These compounds are also present in the heart, lung and brain, suggesting that EM and EG are primarily hypolipidemic in liver, heart, lung and brain tissues. The detection of EM, EG, glucuronide conjugation and sulfate conjugation metabolites in the brain indicates that these metabolites easily pass through the blood–brain barrier, and may be related to the neuro-protective and cognitive effects of EM and EG.

#### Author contributions

JB, XQ and ZH conceived and designed the experiments, JB, QZ HS, and BL performed the experiments and analyzed the data, JB and HZ collected and processed the samples, DZ and LG, contributed reagents/materials/analysis tools, JB wrote the paper.

#### Funding

This work was supported by National Natural Science Foundation of China (81373967, 82204622), Quality standard system construction for the whole industry chain of Chinese medicinal detection pieces from Guangdong Provincial Drug Administration of China (2019KT1261/2020ZDB25).

#### CRediT authorship contribution statement

**Junqi Bai:** Writing – review & editing, Writing – original draft, Resources, Project administration, Methodology, Investigation, Funding acquisition, Formal analysis, Data curation, Conceptualization. **He Su:** Validation, Software. **Baosheng Liao:** Validation, Software, Conceptualization. **Juan Huang:** Methodology, Funding acquisition. **Danchun Zhang:** Methodology, Investigation. **Lu Gong:** Formal analysis, Data curation. **Xuhua Shi:** Data curation. **Zhihai Huang:** Investigation, Funding acquisition. **Xiaohui Qiu:** Project administration, Methodology, Funding acquisition, Formal analysis.

#### Declaration of Competing Interest

The authors declare that they have no known competing financial interests or personal relationships that could have appeared to influence the work reported in this paper.

#### Data availability statement.

The raw data supporting the conclusion of this article will be made available by the authors, without undue reservation.

#### Appendix A. Supplementary data

Supplementary data to this article can be found online at <https://doi.org/10.1016/j.arabjc.2024.105905>.

## References

- Chen, J.F., Song, Y.L., Guo, X.Y., et al., 2014. Characterization of the herb-derived components in rats following oral administration of *Carthamus tinctorius* extract by extracting diagnostic fragment ions (DFIs) in the MSn chromatograms. *Analyst* 139 (24), 6474–6485. <https://doi.org/10.1039/c4an01707b>.
- Cheng, H.L., Chen, J.Y., Zhu, C.Y., et al., 2020. Identification of Emodin Metabolites in vivo by HPLC-HRMS and MMDF Technique [J], pp. 1985–1990+2020 *Mod. Chin. Med.* 22 (12). <https://doi.org/10.13313/j.issn.1673-4890.20190923002>.
- Ding, Y., Zhao, L., Mei, H., et al., 2008. Exploration of Emodin to treat alpha-naphthylisothiocyanate-induced cholestatic hepatitis via anti-inflammatory pathway. *Eur. J. Pharmacol.* 590 (1–3), 377–386. <https://doi.org/10.1016/j.ejphar.2008.06.044>.
- Dong, X., Fu, J., Yin, X., et al., 2016. Emodin: a review of its pharmacology, toxicity and pharmacokinetics. *Phytother. Res.* 30 (8), 1207–1218. <https://doi.org/10.1002/ptr.5631>.
- Ghimire, G.P., Koirala, N., Pandey, R.P., et al., 2015. Modification of emodin and aloe-emodin by glycosylation in engineered *Escherichia coli*. *World J. Microbiol. Biotechnol.* 31, 611–619. <https://doi.org/10.1007/s11274-015-1815-4>.
- Hsu, S.C., Chung, J.G., 2012. Anticancer potential of emodin. *Biomedicine* 2 (3), 108–116. <https://doi.org/10.1016/j.biomed.2012.03.003>.
- Lee, S.U., Shin, H.K., Min, Y.K., et al., 2008. Emodin accelerates osteoblast differentiation through phosphatidylinositol 3-kinase activation and bone morphogenetic protein-2 gene expression. *Int. Immunopharmacol.* 8 (5), 741–747. <https://doi.org/10.1016/j.intimp.2008.01.027>.
- Leung, S.W., Lai, J.H., Wu, J.C.C., et al., 2020. Neuroprotective effects of emodin against ischemia/reperfusion injury through activating ERK-1/2 signaling pathway. *Int. J. Mol. Sci.* 21 (8), 2899. <https://doi.org/10.3390/ijms21082899>.
- Li, L., Song, X., Yin, Z., et al., 2016. The antibacterial activity and action mechanism of emodin from *Polygonum cuspidatum* against *Haemophilus parasuis* in vitro. *Microbiol. Res.* 186, 139–145. <https://doi.org/10.1016/j.micres.2016.03.008>.
- Lin, S.P., Chu, P.M., Tsai, S.Y., Wu, M.H., Hou, Y.C., 2012. Pharmacokinetics and tissue distribution of resveratrol, emodin and their metabolites after intake of *Polygonum cuspidatum* in rats. *J. Ethnopharmacol.* 144 (3), 671–676. <https://doi.org/10.1016/j.jep.2012.10.009>.
- Lin, L., Ni, B., Lin, H., et al., 2015. Traditional usages, botany, phytochemistry, pharmacology and toxicology of *Polygonum multiflorum* Thunb.: a review. *J. Ethnopharmacol.* 159, 158–183. <https://doi.org/10.1016/j.jep.2014.11.009>.
- Mitra, S., Anjum, J., Muni, M., et al., 2022. Exploring the journey of emodin as a potential neuroprotective agent: novel therapeutic insights with molecular mechanism of action. *Biomedicine & Pharmacotherapy* 149, 112877. <https://doi.org/10.1016/j.biopha.2022.112877>.
- Park S Y, M L, Ko M J, et al. Anti-neuroinflammatory effect of emodin in LPS-stimulated microglia: involvement of AMPK/Nrf2 activation[J]. *Neurochemical research*, 2016, 41: 2981-2992. doi: 10.1007/s11064-016-2018-6.
- Shi, X.H., Huang, S.Y., Liang, Y.L., et al., 2021. Emodin-8-O based on UPLC-Q-Exactive MS technology-β-In vivo metabolism of D-glucoside. *J. Chin. Med. Mater.* 44 (10), 2389–2395. <https://doi.org/10.13863/j.issn1001-4454.2021.10.026>.
- Su, Z., Hang, P., Hu, J., et al., 2020. Aloe-emodin exerts cholesterol-lowering effects by inhibiting proprotein convertase subtilisin/kexin type 9 in hyperlipidemic rats. *Acta Pharmacol. Sin.* 41 (8), 1085–1092. <https://doi.org/10.1038/s41401-020-0392-8>.
- Sun, J.H., Yang, M., Han, J.A., et al., 2007. Profiling the metabolic difference of seven tanshinones using high-performance liquid chromatography/multi-stage mass spectrometry with data-dependent acquisition. *Rapid Commun Mass Spectrom* 21 (14), 2211–2226. <https://doi.org/10.1002/rcm.3080>.
- Tian, J., Chen, X., Bai, X.H., 2012. Analysis of emodin and its metabolites based on hollow fiber liquid phase microextraction. *Chin. J. Chroma.* 30 (5), 507–514. <https://doi.org/10.3724/SP.J.1123.2011.12001>.
- Wang, L., Liu, S., Xu, J., et al., 2021. Emodin inhibits aggregation of amyloid-β peptide 1–42 and improves cognitive deficits in Alzheimer's disease transgenic mice. *J. Neurochem.* 157 (6), 1992–2007. <https://doi.org/10.1111/jnc.15156>.
- Wang, Z., Yang, L., Fan, H., et al., 2017. Screening of a natural compound library identifies emodin, a natural compound from *Rheum palmatum* Linn that inhibits DPP4. *PeerJ* 5, e3283.
- Wang, C., Zhang, D., Ma, H., et al., 2007. Neuroprotective effects of emodin-8-O-β-d-glucoside in vivo and in vitro. *Eur. J. Pharmacol.* 577 (1–3), 58–63. <https://doi.org/10.1016/j.ejphar.2007.08.033>.
- Wang, M., Zhang, Z., Ruan, P., et al., 2022. Emodin-induced hepatotoxicity is enhanced by 3-methylcholanthrene through activating aryl hydrocarbon receptor and inducing CYP1A1 in vitro and in vivo. *Chem. Biol. Interact.* 365, 110089 <https://doi.org/10.1016/j.cbi.2022.110089>.
- Wu, L., Chen, Y., Liu, H., et al., 2018. Emodin-induced hepatotoxicity was exacerbated by probenecid through inhibiting UGTs and MRP2. *Toxicol. Appl. Pharmacol.* 359, 91–101. <https://doi.org/10.1016/j.taap.2018.09.029>.
- Wu, S., Zhang, Y., Zhang, Z., Song, R., 2017. Use of liquid chromatography hybrid triple-quadrupole mass spectrometry for the detection of emodin metabolites in rat bile and urine. *Biomed Chromatogr.* 31 (10) <https://doi.org/10.1002/bmc.3979>.